

Development 138, 1913-1923 (2011) doi:10.1242/dev.063966  
 © 2011. Published by The Company of Biologists Ltd

# SHH propagates distal limb bud development by enhancing CYP26B1-mediated retinoic acid clearance via AER-FGF signalling

Simone Probst<sup>1</sup>, Conradin Kraemer<sup>2</sup>, Philippe Demougin<sup>3</sup>, Rushikesh Sheth<sup>1,\*</sup>, Gail R. Martin<sup>4</sup>, Hidetaka Shiratori<sup>5</sup>, Hiroshi Hamada<sup>5</sup>, Dagmar Iber<sup>2</sup>, Rolf Zeller<sup>1</sup> and Aimée Zuniga<sup>1,†</sup>

## SUMMARY

The essential roles of SHH in anteroposterior (AP) and AER-FGF signalling in proximodistal (PD) limb bud development are well understood. In addition, these morphoregulatory signals are key components of the self-regulatory SHH/GREM1/AER-FGF feedback signalling system that regulates distal progression of limb bud development. This study uncovers an additional signalling module required for coordinated progression of limb bud axis development. Transcriptome analysis using *Shh*-deficient mouse limb buds revealed that the expression of proximal genes was distally extended from early stages onwards, which pointed to a more prominent involvement of SHH in PD limb axis development. In particular, retinoic acid (RA) target genes were upregulated proximally, while the expression of the RA-inactivating *Cyp26b1* enzyme was downregulated distally, pointing to increased RA activity in *Shh*-deficient mouse limb buds. Further genetic and molecular analysis established that *Cyp26b1* expression is regulated by AER-FGF signalling. During initiation of limb bud outgrowth, the activation of *Cyp26b1* expression creates a distal 'RA-free' domain, as indicated by complementary downregulation of a transcriptional sensor of RA activity. Subsequently, *Cyp26b1* expression increases as a consequence of SHH-dependent upregulation of AER-FGF signalling. To better understand the underlying signalling interactions, computational simulations of the spatiotemporal expression patterns and interactions were generated. These simulations predicted the existence of an antagonistic AER-FGF/CYP26B1/RA signalling module, which was verified experimentally. In summary, SHH promotes distal progression of limb development by enhancing CYP26B1-mediated RA clearance as part of a signalling network linking the SHH/GREM1/AER-FGF feedback loop to the newly identified AER-FGF/CYP26B1/RA module.

**KEY WORDS:** Fibroblast growth factor, Retinoic acid, Sonic hedgehog, Mathematical modelling, Mouse limb development, Systems biology

## INTRODUCTION

During vertebrate limb bud development, the proximodistal (PD) and anteroposterior (AP) limb skeletal axes develop by proliferative expansion of mesenchymal progenitors in combination with progressive determination and differentiation (Tabin and Wolpert, 2007; Towers and Tickle, 2009; Zeller et al., 2009; Zhu et al., 2008). The apical ectodermal ridge (AER) secretes several fibroblast growth factors (FGFs; FGF4, FGF8, FGF9 and FGF17) that control distal outgrowth and patterning in a likely dose-dependent manner [see e.g. Mariani et al. (Mariani et al., 2008)]. Experimental manipulation of chicken limb bud development has provided evidence that retinoic acid (RA) can

promote proximal fates (Tamura et al., 1997). In particular, implantation of RA-loaded beads into limb buds upregulates the expression of the *Meis* transcriptional regulators, which indicates that they mediate RA signalling in the proximal mesenchyme. *Meis1* and *Meis2* are first expressed throughout the nascent limb bud mesenchyme and their expression becomes restricted proximally during outgrowth. Ectopic expression of *Meis1* in chicken and mouse limb buds causes distal to proximal transformations, whereas implantation of FGF8-loaded beads into the proximal mesenchyme inhibits *Meis* expression (Capdevila et al., 1999; Mercader et al., 1999; Mercader et al., 2000; Mercader et al., 2009). These results led to the two-signal model for PD limb axis patterning, which states that RA from the limb bud flank and FGF signalling by the AER oppose one another to specify proximal and distal limb identities, respectively (Mercader et al., 2000). However, the potential functions of endogenous RA during limb bud morphogenesis have remained largely elusive. RA synthesis requires the RALDH enzymes, whereas its inactivation occurs by CYP26 enzymes, which belong to the cytochrome P450-type enzyme family [see e.g. Yashiro et al. (Yashiro et al., 2004)]. During limb bud development, *Raldh2* is expressed by the flank mesenchyme and genetic analysis provided evidence that it is the RA synthesising enzyme relevant for forelimb bud development (Niederreither et al., 1999). By contrast, *Cyp26b1* is expressed predominantly by the distal mesenchyme and non-AER ectoderm (Yashiro et al., 2004). In *Cyp26b1*-deficient mouse embryos, distal

<sup>1</sup>Developmental Genetics, Department of Biomedicine, University of Basel, Mattenstrasse 28, CH-4058 Basel, Switzerland. <sup>2</sup>Department of Biosystems Science and Engineering (D-BSSE), ETH Zurich, Mattenstrasse 26, CH-4058 Basel, Switzerland. <sup>3</sup>Life Sciences Training Facility, Pharmazentrum, University of Basel, Klingelbergstrasse 50-70, CH-4056 Basel, Switzerland. <sup>4</sup>Department of Anatomy, School of Medicine, University of California at San Francisco, San Francisco, CA 94158-2324, USA. <sup>5</sup>Developmental Genetics Group, Graduate School of Frontier Biosciences, Osaka University, 1-3 Yamada-oka, Suita, Osaka 565-0871, Japan.

\*Present address: Laboratory of Genetics and Development, Institut de Recherches Cliniques de Montréal (IRCM), 110 Avenue des Pins Ouest, H2W 1R7, Montréal, Québec, Canada

†Author for correspondence (aimée.zuniga@unibas.ch)

limb development is disrupted probably owing to the teratogenic effects of elevated RA, which causes cell death and severely truncates the limb skeleton (Yashiro et al., 2004; Zhou and Kochhar, 2004).

Studying the potential requirement of RA for limb bud development has been difficult due to the early lethality of *Raldh2*-deficient mouse embryos and lack of conditional alleles. However, the early lethality can be circumvented by supplementing *Raldh2*-deficient embryos with maternal RA during gastrulation (Niederreither et al., 2002; Zhao et al., 2009). This largely restores forelimb bud outgrowth but AP patterning defects remained, which led the authors to conclude that RA is required for morphogenesis of both limb bud axes (Niederreither et al., 2002). Using a similar approach to restore development of *Raldh2/3*-deficient embryos, Zhao et al. (Zhao et al., 2009) showed that no RA activity is detected in the forelimb bud mesenchyme, although presumed RA targets such as *Meis2*, *Hand2* and *Shh* were expressed. Therefore, this analysis suggested that RA is not required for patterning of the PD axis and hindlimb bud development (Zhao et al., 2009). However, RA appears to inhibit *Fgf8* expression within the trunk mesenchyme, which creates a region competent to form forelimb buds. Prolonged RA-mediated inhibition of FGF8 signalling within the trunk mesenchyme might be required for correct scaling of the forelimb bud size. In addition, genetic analysis in the mouse has implicated mesenchymal FGF10 and BMP4 signalling in formation of the *Fgf8* expressing AER and initiation of limb bud outgrowth (Ohuchi et al., 1997; Benazet et al., 2009).

Sonic hedgehog (SHH) signalling by the limb bud organizer located in the posterior mesenchyme mainly controls establishment of the anteroposterior (AP) limb bud axis, which manifests predominantly in digit identities of the autopod (Chiang et al., 2001; Harfe et al., 2004; Kraus et al., 2001; Zhu et al., 2008). Genetic and experimental manipulation of mouse and chicken limb bud development has revealed the dual role of SHH in the early specification of AP identities and subsequent proliferative expansion (Towers et al., 2008; Zhu et al., 2008). In particular, the descendants of SHH-producing cells in mouse limb buds give rise to the two posterior-most digits and contribute to the middle digit (Harfe et al., 2004). This study provided good evidence that the time cells are exposed to SHH is crucial for specifying posterior identities (digits 3-5), whereas the progenitors of digit 2 are specified by long-range signalling. The upregulation of *Shh* expression over time depends on the BMP antagonist gremlin 1 (GREM1), which is key to establishment of the SHH/GREM1/FGF feedback loop that operates between the mesenchyme and AER (Michos et al., 2004; Zuniga et al., 1999). In fact, GREM1-mediated reduction of BMP4 activity defines a key node in the self-regulatory signalling system that interlinks the SHH, GREM1/BMP4 and AER-FGF signalling pathways in the distal mesenchyme (Benazet et al., 2009; Verheyden and Sun, 2008). Altogether, these studies have revealed that these feedback loops are part of a more complex, as yet only partially identified signalling system that coordinates limb bud axes development (Zeller et al., 2009).

We have investigated the transcriptome alterations between *Shh*-deficient and wild-type forelimb buds around E10.5 (35-36 somites), which corresponds to the period during which limb bud development largely depends on SHH signalling (Benazet et al., 2009; Zhu et al., 2008; Panman et al., 2006). Unexpectedly, this analysis revealed that forelimb buds of *Shh*-deficient mouse embryos were molecularly proximalised as the expression of

several proximal genes was upregulated and their domains extended distally. Molecular analysis of limb buds of *Shh*-, *AER-Fgf*- and *Cyp26b1*-deficient mouse embryos indicated that the decrease in *Cyp26b1* expression and the likely increase in RA activity are the cause for the observed molecular proximalisation of *Shh*-deficient limb buds. Normally, SHH signalling enhances RA inactivation indirectly via AER-FGF-mediated upregulation of *Cyp26b1* expression. These interactions form an integral part of the signalling system that controls distal progression of limb bud development. To gain insight into the potential complexity of the SHH/AER-FGF/RA pathway interactions, a computational model using differential equations based on the observed genetic and molecular interactions was developed. The consistency of the simulations with the in vivo observations could be improved by introducing terms that describe the potential of high RA activity to restrict *Fgf* expression within the AER. The existence of this antagonistic AER-FGF/CYP26B1/RA signalling module was established experimentally. This antagonistic signalling module is established prior to activation of *Shh* expression and becomes dependent on SHH signalling as the SHH/GREM1/FGF feedback loop is initiated. Therefore, both SHH-mediated upregulation of AER-FGF signalling and CYP26B1-mediated RA clearance are key to distal progression of limb and autopod development.

## MATERIALS AND METHODS

### Ethics statement

All studies involving mice were performed in strict accordance with Swiss law after being approved by the Joint Commission on Experiments involving Animals of the Cantons of Argovia and both Basel. All animal experiments were classified as grade zero, which implies minimal suffering of mice and the 3R principles were strictly implemented as required by Swiss law.

### Mouse forelimb bud isolation and Affymetrix Gene Chip analysis

*Shh*-deficient mouse embryos were produced using the previously generated *Shh* loss-of-function mutation (St-Jacques et al., 1998). For the transcriptome analysis, the Affymetrix GeneChip MoGene-1\_0-st-v1 was used, which covers over 28,000 well-annotated mouse transcripts. Three individual pairs of mouse forelimb buds at embryonic day E10.5 of the same genotype and sex were used to isolate total RNA by the RNeasy micro kit (Qiagen). Total RNAs (200 ng) were used to synthesize target cRNA using the WT expression kit (Ambion). cRNAs (10 µg) were used to generate ~8.0 µg (±0.1 µg) of cDNAs. The WT Terminal Labelling Kit (Affymetrix) was used to fragment the cDNAs. The hybridization cocktail (85 µl) containing fragmented and biotin-labelled cDNAs (25 ng/µl) was transferred into Affymetrix GeneChip MoGene-1\_0-st-v1 cassettes, which were incubated at 45°C inside a hybridization oven by rotating them at 60 rpm for 17 hours. Then the GeneChip arrays were washed and developed using the Hybridization Wash and Stain Kit in a Fluidics Station 450. The GeneChip arrays were read using the GeneChip Scanner 3000 7G and DAT image files were generated using the GeneChip Command Console (Affymetrix). Quality control established that the only significant source of variation in expression levels were the genotypes, which provided the experimental basis for validating the significance of the observed differences (data not shown).

The Partek Genomic Suite 6.5 was employed to further validate the GeneChip results. Three completely independent samples for both genotypes were used to determine significant differences in expression levels. All Affymetrix CEL files were normalized using the RMA method and all data were  $\log_2$  transformed. To identify differentially expressed genes, two-way ANOVA analysis based on the 'method of moments' was used. Differentially expressed genes were further filtered using a *P*-value threshold of 0.03 or less. These validated data sets were interrogated further using Ingenuity Pathway analysis in combination with manual curation of particular classes of genes. Microarray data have been submitted to MIAMExpress (Accession Number E-MEXP-3142).

**Real-time quantitative PCR**

Pairs of forelimb buds were collected and cDNAs synthesized using Superscript III (Invitrogen). Transcript levels were quantified by real-time PCR using the BIO-RAD CFX96 Real Time System in combination with the iQ-SYBR<sup>+</sup>Green Supermix (BioRad; primer sequences available upon request). Relative transcript levels were normalized using the levels of the hydroxymethylbilane synthase gene as an internal standard. Transcript levels in mutant forelimb buds were calculated relative to wild-type levels (average set to 100%). All results shown are based on analysing 7-10 pairs of forelimb buds per genotype ( $\pm$ s.d.). The statistical significance of all results was assessed using the two-tailed, non-parametric Mann-Whitney test.

**Culturing of mouse limb buds**

Mouse forelimb buds were cultured as described (Panman et al., 2006). AG1-X2 beads were loaded with RA (1 mg/ml, dissolved in DMSO) or the retinoid antagonist BMS493 (2 mg/ml, dissolved in DMSO; InnoChemie). Heparin beads were loaded with recombinant FGF4 (1 mg/ml in PBS/0.1% BSA; from R&D Systems). FGF signal transduction was blocked by supplementing the culture medium with 10  $\mu$ M SU5402 (dissolved in DMSO) (Zuniga et al., 2004).

**Whole-mount RNA in situ hybridization**

Digoxigenin-labelled antisense riboprobes were used for whole-mount RNA in situ hybridization (Panman et al., 2006). Minimally three, but often many more, independent embryos were analysed and yielded comparable results for all results shown.

The mathematical approaches underlying the spatio-temporal simulations of the signalling systems interactions (Figs 7, 8) are described in Appendix S1 (see supplementary material).

**RESULTS****Transcriptome alterations in *Shh*-deficient mouse limb buds**

Recent studies have revealed the dual function of SHH in specification and proliferative expansion of the autopod primordia (Zhu et al., 2008). To gain insight into how SHH regulates gene expression during limb bud development, we have profiled the transcriptome in *Shh*-deficient mouse forelimb buds (St-Jacques et

al., 1998) using Affimetrix GeneChip Mouse Gene Arrays. Forelimb buds of *Shh*-deficient mouse embryos at E10.5 (35-36 somites) were chosen because they are of similar size to wild-type limb buds and display neither morphological changes nor massive cellular apoptosis. At this developmental stage, the progression of limb bud development and proliferative expansion of the autopod primordia are mainly controlled by the SHH/GREM1/FGF signalling system (Benazet et al., 2009; Panman et al., 2006). Statistical evaluation of the primary results revealed that  $\sim$ 800 transcripts were altered at least 1.2-fold in *Shh*-deficient forelimb buds ( $P < 0.03$ ) (see Tables S1, S2 in the supplementary material). The cut-off was set at 1.2, as such differences were reliably detected by RNA in situ hybridization and real-time PCR analysis (Figs 1, 2). This group contained a large number of known transcriptional targets of SHH signalling [such as *Ptch1*, *Ptch2*, *Hhip*, *Gli1*; the 5'*Hoxd* genes, *Grem1*, *Hand2*, *Prdm1* and AER-*Fgf4*, *Fgf8*, *Fgf9* (see Table 1); *Gas1*, *Boc*, *Cdon* and *Displ1* (see Table 2) (Chiang et al., 2001; te Welscher et al., 2002; Vokes et al., 2008; Zuniga et al., 1999)]. In addition,  $\sim$ 400 genes were downregulated  $\geq 1.2$ -fold in *Shh*-deficient limb buds, consistent with a positive role of SHH in gene expression. Systematic annotation in combination with RNA in situ hybridization analysis showed that the majority of these genes are normally expressed in the posterior and/or distal limb bud mesenchyme or the AER (Table 1, Fig. 1A-C). In *Shh*-deficient limb buds, their expression was lowered rather than the spatial distribution altered, as illustrated for selected genes such as *Wnt5a* (Fig. 1A) (Yamaguchi et al., 1999), *Spry4* (Fig. 1B) (Minowada et al., 1999) and *Sall1* (Fig. 1C) (Kawakami et al., 2009). This rather general reduction of transcription in the distal mesenchyme and AER (Table 1) preceded the massive apoptosis in *Shh*-deficient limb buds (data not shown). Furthermore, the expression of components of the cell-cycle and proliferation gene networks were altered in a manner consistent with the G1 cell-cycle arrest observed in *Shh*-deficient limb buds [Zhu et al. (Zhu et al., 2008) and data not shown].

**Table 1. Classification and spatial distribution of genes downregulated in *Shh*-deficient limb buds**

A	Posterior	Posterior-distal	Distal				
B Genes downregulated in <i>Shh</i> -deficient limb buds							
Gene	FC	<i>P</i> -value	Distribution	Gene	FC	<i>P</i> -value	Distribution
<i>Hoxa13</i>	4.9	$\leq 4.8 \times 10^{-5}$	Distal	<i>Rspo3</i>	2.1	$\leq 3.7 \times 10^{-5}$	Post-distal
<i>Sall1</i>	2.9	$\leq 6.2 \times 10^{-5}$	Distal	<i>Evx1</i>	1.3	$\leq 5.9 \times 10^{-3}$	Post-distal
<i>Sall3</i>	1.9	$\leq 1.2 \times 10^{-2}$	Distal	<i>Fmn1</i>	1.2	$\leq 7.7 \times 10^{-3}$	Post-distal
<i>Cyp26b1</i>	1.7	$\leq 1.4 \times 10^{-3}$	Distal	<u><i>Ptch2</i></u>	5.7	$\leq 5.9 \times 10^{-5}$	Posterior
<i>Sall4</i>	1.7	$\leq 1.4 \times 10^{-2}$	Distal	<u><i>Ptch1</i></u>	4.4	$\leq 6.8 \times 10^{-6}$	Posterior
<i>Spry4</i>	1.6	$\leq 2.0 \times 10^{-2}$	Distal	<u><i>Gli1</i></u>	3.8	$\leq 1.2 \times 10^{-5}$	Posterior
<i>Hey1</i>	1.6	$\leq 1.7 \times 10^{-3}$	Distal	<i>Hhip</i>	2.7	$\leq 3.5 \times 10^{-4}$	Posterior
<i>Jag1</i>	1.5	$\leq 9.8 \times 10^{-3}$	Distal	<i>Hand2</i>	2.6	$\leq 1.6 \times 10^{-4}$	Posterior
<i>Sost</i>	1.5	$\leq 3.0 \times 10^{-3}$	Distal	<i>Cyp1b1</i>	1.8	$\leq 7.0 \times 10^{-4}$	Posterior
<i>Wnt5a</i>	1.3	$\leq 2.8 \times 10^{-3}$	Distal	<i>Bmp2</i>	1.3	$\leq 1.8 \times 10^{-2}$	Posterior
<i>Hes1</i>	1.3	$\leq 1.4 \times 10^{-2}$	Distal	<i>Cdc25b</i>	1.3	$\leq 2.8 \times 10^{-2}$	Posterior
<i>Slit3</i>	1.3	$\leq 2.4 \times 10^{-2}$	Distal	<i>Osr1</i>	2.6	$\leq 3.2 \times 10^{-3}$	Prox-post
<i>Hoxd13</i>	20	$\leq 6.7 \times 10^{-7}$	Post-distal	<i>Fgf4</i>	2.7	$\leq 4.9 \times 10^{-4}$	AER
<i>Hoxd12</i>	17	$\leq 4.3 \times 10^{-5}$	Post-distal	<i>Fgf8</i>	2	$\leq 8.7 \times 10^{-3}$	AER
<i>Grem1</i>	3.7	$\leq 3.0 \times 10^{-5}$	Post-distal	<i>Fgf9</i>	1.5	$\leq 1.0 \times 10^{-2}$	AER

(A) The limb bud schemes define graphically what are considered 'posterior', 'posterior-distal' and 'distal' expression domains. (B) Known transcriptional targets of the SHH signalling pathway are underlined. FC, fold change; post, posterior; prox, proximal.

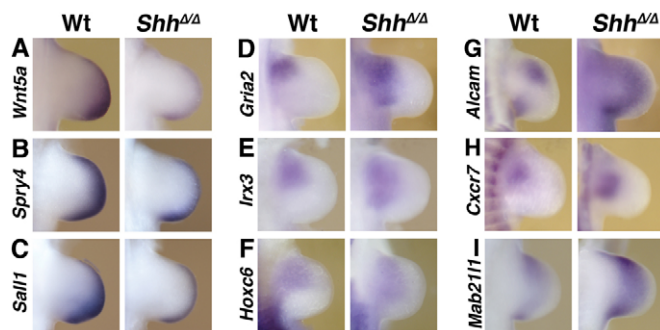


**Fig. 1. Spatial alterations of the expression domains of selected genes in *Shh*-deficient limb buds (E10.5; 34-36 somites).** (A-C) The expression of distal genes is generally reduced in *Shh*-deficient (*Shh*<sup>ΔΔ</sup>) limb buds in comparison with wild types (Wt). (A) *Wnt5a*, (B) *Spry4* and (C) *Sall1*. (D-F) Representative alterations of the spatial expression domains of proximal-anterior genes that are upregulated in *Shh*-deficient limb buds. (D) *Gria2*, (E) *Irx3* and (F) *Hoxc6*. (G-I) The expression of a third group of genes is normally restricted proximally, but in *Shh*-deficient limb buds their expression domains are enlarged and/or extended distally. (G) *Alcam*, (H) *Cxcr7* and (I) *Mab211l*.

### Upregulation of genes expressed in the proximal and proximal-anterior mesenchyme in *Shh*-deficient limb buds

Initially rather unexpected, the expression of a roughly equal number of genes was upregulated in *Shh*-deficient limb buds at E10.5. Annotation revealed that at least 36 of these upregulated genes were expressed proximally, and about half were restricted to the proximal-anterior mesenchyme in wild-type forelimb buds (Table 2). The expression of anteriorly restricted genes extended posteriorly in *Shh*-deficient limb buds as shown for *Gria2*, *Irx3* and *Hoxc6* (Fig. 1D-F) (Houweling et al., 2001; Jia et al., 1996; Nelson et al., 1996). Furthermore, *Alcam* is expressed in two distinct mesenchymal domains in wild-type limb buds (Bowen et al., 1995), but this restricted localization was lost in *Shh*-deficient limb buds (Fig. 1G). The distally extended expression of *Cxcr7* (Maksym et al., 2009) is representative for the spatial alterations of many proximal genes in *Shh*-deficient mouse limb buds (Fig. 1H). In wild-type limb buds, *Mab211l* (Wong et al., 1999) is expressed in a medial mesenchymal stripe (left panel, Fig. 1I). This indicated that the *Mab211l* expression domain could mark the presumptive zeugopodal domain like *Hoxa11* (Zakany and Duboule, 2007). In *Shh*-deficient limb buds, *Mab211l* expression was upregulated and distally extended (right panel, Fig. 1I). Taken together, this analysis reveals that the expression of proximal genes was distally extended in *Shh*-deficient limb buds, which shows that SHH signalling is required for the correct proximal restriction of their expression domains during limb bud outgrowth.

### Proximalization of *Shh*-deficient limb buds is paralleled by increased RA activity

The molecular alterations described so far indicated that *Shh*-deficient limb buds (E10.0-E10.5) were molecularly proximalized. One of the affected genes was the RA receptor *Rarb* (Fig. 2A), which serves as a sensor for RA activity as its expression is positively regulated by RA [see e.g. Zhao et al. (Zhao et al., 2009)]. Normally, *Rarb* expression is restricted to the proximal part of the limb bud with highest levels in the most anterior and posterior mesenchyme (left panel, Fig. 2A). In *Shh*-deficient limb buds, its expression was distally extended (middle panel, Fig. 2A) and levels

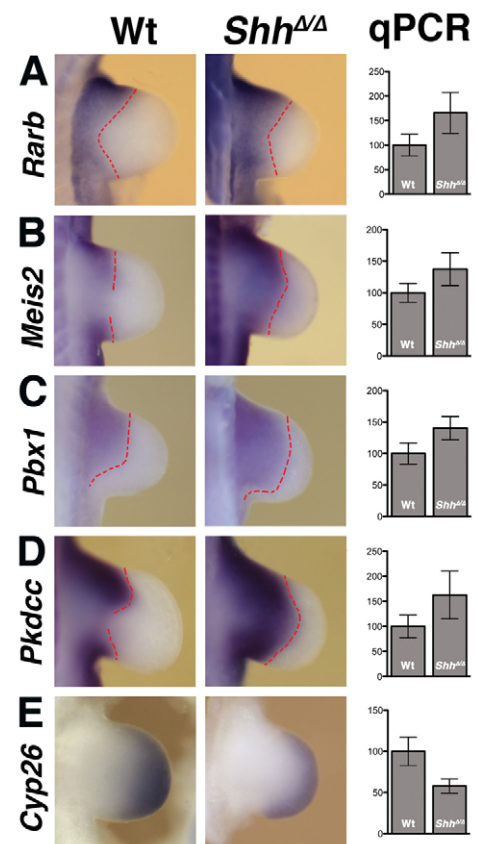


**Fig. 2. RA pathway alterations in *Shh*-deficient limb buds.** RA target genes are upregulated and extended distally in *Shh*-deficient (*Shh*<sup>ΔΔ</sup>) limb buds (E10.5; 34-36 somites). (A) *Rarb*, (B) *Meis2*, (C) *Pbx1*, (D) *Pkdcc* and (E) *Cyp26b1* (*Cyp26*) expression in wild-type (Wt, left panels) and *Shh*-deficient forelimb buds (middle panels). The broken red lines demarcate the distal limit of the expression domains. Quantitative real-time PCR (qPCR) was used to determine the relative expression levels in limb buds ( $n=7$  limb bud pairs at E10.5, 35-36 somites, right panels). Mean  $\pm$  s.d. is shown. All differences between wild-type (Wt) and *Shh*-deficient limb buds are significant ( $P<0.001$ , except  $P<0.01$  for *Meis2*).

were increased  $\sim 50\%$  (right panel, Fig. 2A), which indicated that RA activity might be increased in *Shh*-deficient limb buds. Indeed, the expansion of *Rarb* expression was paralleled by *Meis2*, an established transcriptional target of RA signalling in the proximal limb bud mesenchyme (Fig. 2B) (Mercader et al., 1999; Mercader et al., 2000). In *Shh*-deficient limb buds, *Meis2* expression extended distally and levels were increased by  $\sim 40\%$  (Fig. 2B). In addition, we identified two novel potential RA target genes whose expression is normally restricted proximally in limb buds (Fig. 2C,D; see Fig. S1 in the supplementary material). *Pbx1* is expressed in the proximal-anterior part of wild-type limb buds (Selleri et al., 2001). In *Shh*-deficient limb buds, its expression extended both distally and posteriorly (Fig. 2C). *Pkdcc* encodes a putative protein kinase (Imuta et al., 2009) and in wild-type limb buds its expression was restricted proximally, while it was distally extended in *Shh*-deficient limb buds (Fig. 2D; similar to *Meis2*). In addition, *Pbx1* and *Pkdcc* transcript levels were significantly upregulated in *Shh*-deficient limb buds (Fig. 2C,D). To determine if these transcriptional alterations could be a consequence of increased RA activity, RA-loaded beads were

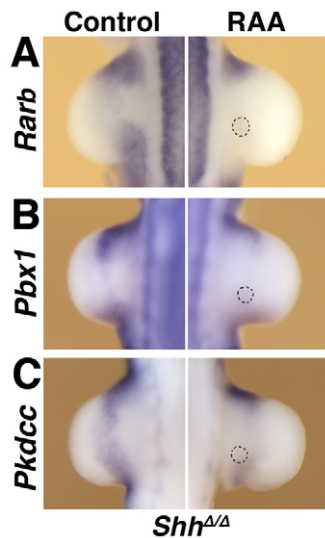


**Fig. 3. Implants of RA antagonist-loaded beads reduce the expression of proximal genes in *Shh*-deficient limb buds.** *Shh*-deficient forelimb buds (E10.5; 34–36 somites) were cultured for 16–20 hours following implantation of a carrier bead loaded with 2 mg/ml RA antagonist (RAA; dotted circle). The non-grafted contralateral forelimb bud is shown in the left panels. Expression of the proximal genes (A) *Rarb* ( $n=7/8$ ), (B) *Pbx1* ( $n=5/6$ ) and (C) *Pkdcc* ( $n=5/6$ ) is reduced following implantation of an RAA bead.

implanted into wild-type mouse forelimb buds, which indeed suffices to distally extend the expression domains of *Meis2*, *Pbx1* and *Pkdcc* (see Fig. S1 in the supplementary material).

To further substantiate the hypothesis that increased RA pathway activity could underlie the proximalization of *Shh*-deficient forelimb buds, the transcriptome alterations were interrogated for changes in components of the RA pathway and target genes. Indeed, significant alterations were seen (see Table S3 in the supplementary material). In particular, the expression of *Cyb26b1* was reduced ~1.7 fold in the distal mesenchyme of *Shh*-deficient mouse limb buds (Fig. 2E). CYP26B1 converts RA to its hydroxylated, inactive form (MacLean et al., 2001). This decrease in *Cyp26b1* expression provides a plausible mechanistic explanation for the suspected increase in RA activity and distally extended expression domains of RA responsive genes in *Shh*-deficient limb buds. Furthermore, beads loaded with a RA antagonist (RAA) (Mercader et al., 2000) were implanted into *Shh*-deficient and wild-type limb buds in culture (Fig. 3; see Fig. S1 in the supplementary material). Such inhibition of RA activity indeed reduced the expression of *Rarb*, *Pbx1* and *Pkdcc* in *Shh*-deficient limb buds, which indicated that their altered expression could be a consequence of increased RA activity (Fig. 3). Taken together, this analysis indicates that decreased *Cyp26b1* expression results in increased RA activity, which probably underlies the molecular proximalization of *Shh*-deficient limb buds.

### ***Cyb26b1* expression in the distal limb bud depends critically on AER-FGF signalling**

Next, we sought to determine the cause of the decreased *Cyp26b1* expression in *Shh*-deficient limb buds. In particular, we considered the possibility that this decrease could be linked to the  $\geq 50\%$

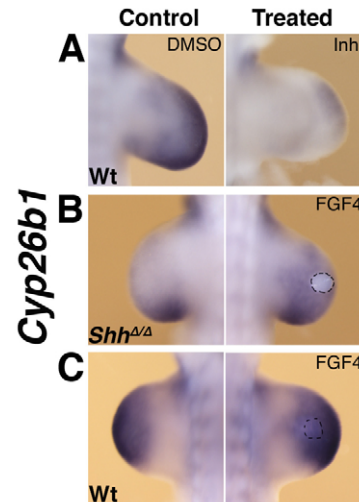


**Fig. 4. FGF4 upregulates *Cyp26b1* expression.** All panels show *Cyp26b1* expression in wild-type (A,C) and *Shh*-deficient (B) limb buds. Left panels show non-treated and/or contralateral control forelimb buds, right panels show experimental forelimb buds. (A) Wild-type limb bud cultured in presence of 10  $\mu$ M SU5402, an inhibitor of FGF signal transduction (Inh.) for 16–20 hours. Controls were cultured in medium supplemented with the solvent DMSO. (B) Implantation of a FGF4-loaded bead (1 mg/ml) into a *Shh*-deficient forelimb bud. *Cyp26b1* expression was analysed after 16–20 hours of culture. (C) Implantation of an FGF4-loaded bead (1 mg/ml) into a wild-type limb bud (16–20 hours culture). The dotted circles indicate the implanted beads.

overall reduction of AER-*Fgf* expression (Table 1) (Chiang et al., 2001; Zuniga et al., 1999). Indeed, culturing of wild-type forelimb buds in the presence of an inhibitor of the FGF receptor tyrosine kinase (SU5402) (Zuniga et al., 2004) resulted in almost complete loss of *Cyp26b1* expression (Fig. 4A). Conversely, the implantation of FGF4-loaded beads into *Shh*-deficient limb buds resulted in striking restoration of *Cyp26b1* expression (Fig. 4B). By contrast, the implantation of FGF4-loaded beads into wild-type limb buds caused only a modest increase, which indicates that *Cyp26b1* is probably expressed at close to maximal levels in wild-types (Fig. 4C). These manipulations established that increased FGF signalling was sufficient to restore *Cyp26b1* expression in the absence of SHH, which reveals that the reduction in AER-FGF signalling (Table 1) (Zuniga et al., 1999) is the likely cause of reduced *Cyp26b1* expression in *Shh*-deficient limb buds.

To further investigate the role of AER-FGFs in regulation of *Cyp26b1* expression, we analyzed forelimb buds with reduced AER-FGF signalling. In AER-*Fgf*<sup>mut</sup> limb buds, the *Fgf8* and *Fgf4* loci are conditionally inactivated in the AER by the *Msx2*-Cre transgene. In addition, AER-*Fgf*<sup>mut</sup> limb buds are heterozygous for a *Fgf9*-null allele. In the AER of mutant forelimb buds there is early but transient expression of both *Fgf4* and *Fgf8*, which supports the development of proximal but not distal skeletal structures (Mariani et al., 2008). This significant genetic reduction in AER-*Fgf* expression results in much more distally restricted expression of *Cyp26b1* than in wild-type and *Shh*-deficient forelimb buds (Fig. 5B; compare with Fig. 5A and 5C), which corroborates the proposed positive regulation of *Cyb26b1* by AER-FGFs. Furthermore, the expression of the RA transcriptional targets *Rarb* and *Pbx1* was extended distally in AER-*Fgf*<sup>mut</sup> forelimb buds (Fig. 5E,H) compared with wild-type and *Shh*-deficient forelimb buds (Fig. 5D,F,G,I).

Table 2. Classification and spatial distribution of genes upregulated in *Shh*-deficient limb buds

A	Proximal	Anterior	Proximal-anterior				
							
B Genes upregulated in <i>Shh</i> -deficient limb buds							
Gene	FC	P-value	Distribution	Gene	FC	P-value	Distribution
<i>Gria2</i>	2.1	$\leq 1.0 \times 10^{-2}$	Prox-ant	<i>Angptl1</i>	2.1	$\leq 1.7 \times 10^{-3}$	Prox
<i>Hoxc5</i>	1.9	$\leq 9.5 \times 10^{-3}$	Prox-ant	<i>Pitx2</i>	1.8	$\leq 1.2 \times 10^{-2}$	Prox
<i>Igf1</i>	1.8	$\leq 7.0 \times 10^{-3}$	Prox-ant	<i>Wif1</i>	1.5	$\leq 7.6 \times 10^{-3}$	Prox
<i>Alx4</i>	1.8	$\leq 1.5 \times 10^{-6}$	Prox-ant	<i>Angptl4</i>	1.5	$\leq 3.9 \times 10^{-4}$	Prox
<i>Pax1</i>	1.7	$\leq 2.5 \times 10^{-2}$	Prox-ant	<i>Glis1</i>	1.5	$\leq 4.9 \times 10^{-3}$	Prox
<i>Irx3</i>	1.6	$\leq 5.2 \times 10^{-5}$	Prox-ant	<i>Zfmx4</i>	1.4	$\leq 1.6 \times 10^{-3}$	Prox
<i>Irx5</i>	1.6	$\leq 1.1 \times 10^{-4}$	Prox-ant	<i>Hand1</i>	1.4	$\leq 1.9 \times 10^{-3}$	Prox
<i>Alx3</i>	1.5	$\leq 2.1 \times 10^{-3}$	Prox-ant	<i>Rarb</i>	1.3	$\leq 3.9 \times 10^{-4}$	Prox
<i>Efna3</i>	1.5	$\leq 1.2 \times 10^{-3}$	Prox-ant	<i>Met</i>	1.3	$\leq 2.8 \times 10^{-2}$	Prox
<i>Zfmx3</i>	1.4	$\leq 7.2 \times 10^{-3}$	Prox-ant	<i>Mab2111</i>	1.2	$\leq 1.8 \times 10^{-3}$	Prox
<i>Efna5</i>	1.4	$\leq 4.2 \times 10^{-4}$	Prox-ant	<i>Meis1</i>	1.2	$\leq 3.5 \times 10^{-3}$	Prox
<u><i>Gas1</i></u>	1.3	$\leq 3.0 \times 10^{-4}$	Prox-ant	<i>Pkdcc</i>	1.2	$\leq 5.6 \times 10^{-3}$	Prox
<i>Epb4.113</i>	1.3	$\leq 1.3 \times 10^{-2}$	Prox-ant	<i>Epha7</i>	1.2	$\leq 8.2 \times 10^{-3}$	Prox
<i>Glis3</i>	1.3	$\leq 5.3 \times 10^{-3}$	Prox-ant	<i>Meis2</i>	1.2	$\leq 2.3 \times 10^{-4}$	Prox
<u><i>Cdon</i></u>	1.3	$\leq 4.9 \times 10^{-3}$	Prox-ant	<i>Hoxb9</i>	1.5	$\leq 2.8 \times 10^{-2}$	Ant
<i>Boc</i>	1.3	$\leq 1.2 \times 10^{-3}$	Prox-ant	<i>Col1a2</i>	1.4	$\leq 2.1 \times 10^{-3}$	Ant
<i>Pbx1</i>	1.3	$\leq 2.4 \times 10^{-2}$	Prox-ant	<u><i>Disp1</i></u>	1.3	$\leq 1.6 \times 10^{-3}$	Ant
<i>Hoxc6</i>	1.3	$\leq 1.9 \times 10^{-2}$	Prox-ant	<i>Sox6</i>	1.3	$\leq 6.0 \times 10^{-3}$	Ant
<i>Pbx3</i>	1.2	$\leq 3.7 \times 10^{-3}$	Prox-ant	<i>Msx2</i>	1.8	$\leq 9.0 \times 10^{-4}$	High ant/Low post
<i>Efnb2</i>	1.2	$\leq 3.5 \times 10^{-2}$	Prox-ant	<i>Igfbp5</i>	1.5	$\leq 9.6 \times 10^{-4}$	AER
<i>Epha3</i>	1.7	$\leq 1.6 \times 10^{-2}$	Prox-ant/prox-post	<i>Dlx5</i>	1.4	$\leq 1.1 \times 10^{-2}$	AER
<i>Slit2</i>	1.4	$\leq 2.2 \times 10^{-2}$	Prox-ant/prox-post	<i>Dlx3</i>	1.2	$\leq 2.4 \times 10^{-5}$	AER

(A) The limb bud schemes define graphically what are considered 'proximal', 'anterior' and 'proximal-anterior' expression domains. (B) Known transcriptional targets of the SHH signalling pathway are underlined. FC, fold change; ant, anterior; post, posterior; prox, proximal.

In *Cyp26b1*-deficient limb buds (Yashiro et al., 2004), the expression of all RA targets investigated was extended very distally (Fig. 5J-L). The extent of molecular proximalization was rather similar in *Cyp26b1*-deficient and AER-*Fgf*<sup>mut</sup> forelimb buds, but less severe in *Shh*-deficient limb buds. In particular, the distal expansion of *Rarb* expression in *Cyp26b1*-deficient and AER-*Fgf*<sup>mut</sup> limb buds was indicative of ectopic RA activity in the distal mesenchyme (Fig. 5E,J; compare with 5D). Taken together, these results indicate that distal progression of limb bud development not only depends on AER-FGF and SHH signalling as part of the SHH/GREM1/AER-FGF feedback loop, but also on CYP26B1-mediated RA clearance.

### The early activation of *Cyb26b1* indicates molecular specification of a distal domain within the nascent limb bud mesenchyme

Next, we assessed the temporal relationship between the expression of *Rarb*, *Cyp26b1* and *Fgf8*, the first AER-*Fgf* expressed during limb bud development and investigated when the regulation of *Cyp26b1* expression by AER-FGFs would become SHH dependent. The expression of *Rarb* was first detected throughout the nascent limb bud mesenchyme, but decreased concurrent with activation of *Cyp26b1* expression in the distal-most mesenchyme (Fig. 6A,B). This suggested that the onset of CYP26B1-mediated RA inactivation creates a 'RA-free' domain within the distal limb bud mesenchyme. *Fgf8* is expressed by the nascent AER (Fig. 6C) from the initiation of forelimb bud development onwards (embryonic day  $\leq$ E9.0) (Sun et al., 2002) together with its transcriptional target *Spry4* in the mesenchyme (Fig. 6D)

(Minowada et al., 1999). In contrast to *Spry4*, *Cyp26b1* expression was always rather distally restricted (Fig. 6B,D). *Cyp26b1* expression increased in parallel to AER-FGF signal transduction and remained complementary to the *Rarb* expression domain ( $\leq$ E9.5; Fig. 6E-H). These expression patterns delineate a proximal (*Rarb*) and distal (*Cyb26b1*) domain, even during early initiation of limb bud outgrowth. In parallel, SHH signalling is activated (Platt et al., 1997), but no alterations in *Rarb* and *Cyb26b1*/AER-*Fgf8* expression were detected in *Shh*-deficient limb buds at these early stages (Fig. 6I-L). Therefore, the initial upregulation of *Cyp26b1* expression and molecular definition of proximal and distal domains are independent of SHH signalling. The expression of *Rarb*, *Cyp26b1* and AER-*Fgfs* started to be altered in *Shh*-deficient limb (see Fig. S2 in the supplementary material) only during the time period when the SHH/GREM1/AER-FGF signalling system becomes operational in wild-type limb buds ( $\sim$ E10.0) (Michos et al., 2004; Chiang et al., 2001; Zuniga et al., 1999).

### Spatiotemporal simulations of the genetically verified interactions reveal an antagonistic signalling module

The simplest signalling module that could be derived from the genetic and functional analysis is shown in Fig. 7A. Mathematical simulations were used to determine if this module would be sufficient to explain the molecular alterations observed in *Shh*-deficient limb buds. Previously, we had succeeded in simulating the temporal dynamics of the SHH/GREM1/AER-FGF feedback signalling system (Benazet et al., 2009). However, as spatial

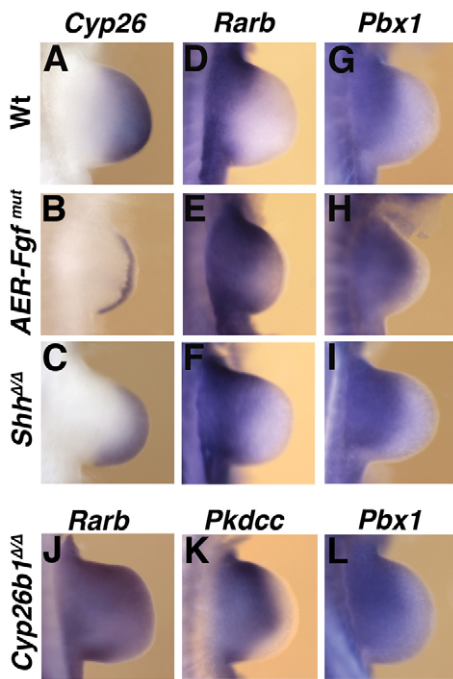


**Fig. 5. Similar alterations in the expression of selected RA pathway genes in *Shh*, *Fgf* and *Cyp26b1* mutant limb buds.** Comparative expression analysis of (A-C) *Cyp26b1*, (D-F,J) *Rarb*, (G-I,L) *Pbx1* and (K) *Pkdcc* in wild-type (Wt), *AER-Fgf<sup>mut</sup>*, *Shh*-deficient and *Cyp26b1*-deficient forelimb buds (E10.5; 34-35 somites). *AER-Fgf<sup>mut</sup>* forelimb buds are of the following genotype: *Msx2-Cre<sup>Tg/+</sup>;Fgf4<sup>Δflox</sup>, Fgf8<sup>Δflox</sup>, Fgf9<sup>Δ/+</sup>*.

aspects are key to the interactions studied here, we solved a set of reaction-diffusion type partial differential equations on a growing 2-dimensional (2D) domain, which represented an idealized limb bud domain (for details see Appendix S1 in the supplementary material). The spatial expression/activity levels were simulated over time and are shown at specific developmental time points. To enable easier comparison with the in vivo gene expression domains, the simulated spatial distributions and activity levels were projected onto the growing 2D limb bud domain (Fig. 7B). The initial simulations reproduced the in vivo *Rarb* and *Cyp26b1* expression domains in wild-type limb buds to some extent (Fig. 7C; compare with Figs 5, 6). By contrast, *Fgf8* expression, which is indicative of AER length did not match the *AER-Fgf8* expression pattern observed in vivo as it extended very proximally in the simulation (Fig. 7C). The match between simulations and in vivo expression domains could be significantly improved by postulating that high RA levels inhibit *AER-Fgfs* (Fig. 8A,B). This prediction was supported indirectly by two previous experimental observations: (1) beads loaded with high levels of RA were able to inhibit AER formation in chicken limb buds (Tickle et al., 1989); and (2) *AER-Fgf4* but not *Fgf8* expression was reduced in *Cyp26b1*-deficient mouse limb buds (Yashiro et al., 2004). To establish that RA is indeed able to inhibit *AER-Fgf* expression, beads loaded with high levels of RA were implanted into the distal mesenchyme of wild-type mouse limb buds in culture (Fig. 8C,D). These experiments revealed that RA inhibited *AER-Fgf8* and *Fgf4* expression differentially. The *Fgf8* expression was reduced only in close proximity to the RA-loaded bead (Fig. 8C), whereas *Fgf4*

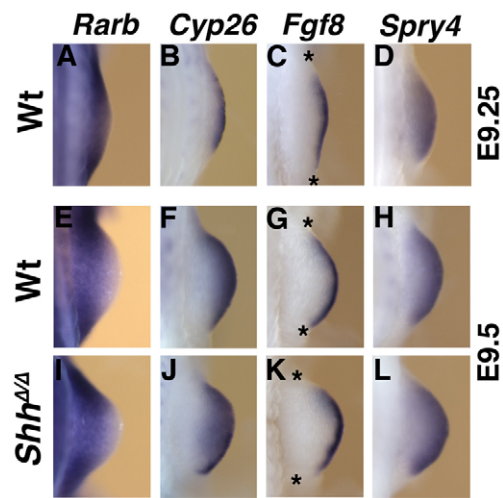


**Fig. 6. Molecular evidence for the early and SHH-independent establishment of a distal limb bud mesenchymal domain.** (A-H) Expression of *Rarb*, *Cyp26b1*, *Fgf8* and *Spry4* in wild-type forelimb buds at E9.25 (A-D; 23 somites) and E9.5 (E-H; 25-26 somites). *Cyp26b1* expression is already detected in the distal-most mesenchyme during initiation of limb bud development (E9.25, B). (I-L) Expression of the same genes in *Shh*-deficient forelimb buds at E9.5. The complementary domains of *Rarb* and *Cyp26b1*, and the expression of *AER-Fgf8* and *Spry4* are not yet altered in *Shh*-deficient forelimb buds. Asterisks indicate the anterior and posterior margins of forelimb buds.

was reduced throughout the AER (Fig. 8D). Furthermore, the expression of *Spry4* was also reduced (Fig. 8D). These results corroborate the proposal that high RA activity inhibits *AER-Fgf* expression and the antagonistic nature of the RA/*AER-FGFs* interactions. The antagonistic *AER-FGF/CYP26B1/RA* signalling module (Fig. 8A) probably serves (1) to restrict *AER-Fgf8* expression and (2) to define molecularly a distal RA-free mesenchymal region during initiation of limb bud outgrowth (Fig. 6).

When we incorporated the ~12 hours delayed input of the SHH/GREM1/*AER-FGF* feedback loop (right panel, Fig. 8B; see Fig. S2 in the supplementary material) (Lewandoski et al., 2000; Michos et al., 2004; Zuniga et al., 1999) into the corresponding equations, the simulations rather accurately reproduced the spatiotemporal changes of the *Rarb*, *Cyp26b1* and *AER-Fgf* expression patterns in wild-type (Fig. 8E; compare with Figs 5, 6) and *Shh*-deficient mouse limb buds (Fig. 8F; compare with Fig. 2; Fig. S2 in the supplementary material). In particular, *Cyp26b1* expression was reduced concurrent with the disruption in the increase in *AER-Fgfs* in simulations of *Shh*-deficient limb buds. This resulted in distal expansion of *Rarb* expression (Fig. 8F), which reproduced the observed increase in RA activity and molecular proximalization of *Shh*-deficient mouse limb buds (Fig. 2, Table 2). When *Cyp26b1* expression was set to zero to simulate the *Cyp26b1* deficiency, *Rarb* levels were more increased and *AER-Fgf* levels more decreased (see Fig. S3 in the supplementary material) than observed in *Cyp26b1*-deficient mouse limb buds (Fig. 5J-L). Yashiro et al. (Yashiro et al., 2004) suggested that precocious activation of *Cyp26a1* could to some extent compensate the *Cyp26b1* deficiency. Indeed, when the expression of the RA-inactivating enzymes was reduced to only 45% to mimic partial functional compensation, the simulations of

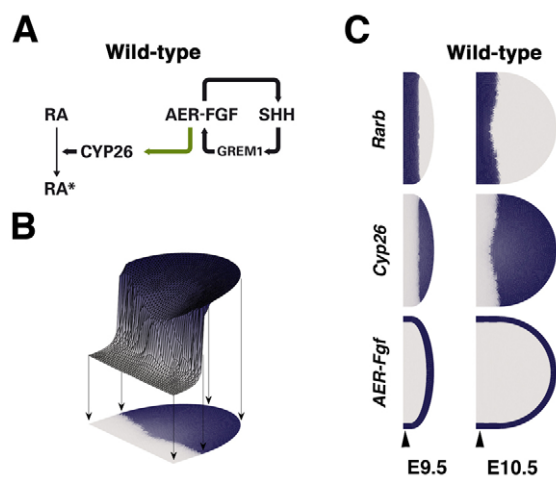


**Fig. 7. Towards spatiotemporal simulations of the AER-FGF/CYP26B1/RA signalling interactions.** (A) Scheme of the gene network derived from the genetic and experimental analysis of the regulatory interactions. This network was initially used to define the partial differential equations and simulate the gene expression domains and interactions. RA inactivation by CYP26B1-mediated hydroxylation is indicated by an asterisk (RA\*). The green arrow indicates the positive regulation of *Cyp26b1* expression by AER-FGF signalling. SHH signalling upregulates *Cyp26b1* expression indirectly via its positive effect on AER-Fgf expression as part of the SHH/GREM1/AER-FGF feedback loop. (B) Illustration of how the simulation of the spatial distribution of *Cyp26b1* levels is projected onto a schematic 2D limb bud domain. (C) Based on this initial network, the dynamic spatial distributions of RA activity (*Rarb*), *Cyp26b1* and AER-Fgfs were simulated in a growing domain for wild-type limb buds. The simulated AER-Fgf expression domain extends to the proximal limb bud margin (arrowheads). Activity levels are represented by a colour code such that dark blue corresponds to high and white to no activity. All limb bud schemes are oriented with proximal towards the left and anterior towards the top.

*Cyp26b1*-deficient limb buds matched the in vivo observed alterations much better. For example, the expression of AER-Fgf activity was initially normal, but reduced later (see Fig. S3 in the supplementary material), which mimics the observed reduction of *Fgf4* during mouse limb bud outgrowth (Yashiro et al., 2004). These simulations indicate that the partial redundancy among *Cyp26* family members might be of functional relevance to limb bud development, as is the case during primary body axis development (Uehara et al., 2009). Taken together, these simulations (Fig. 8E,F and see Fig. S3 in the supplementary material) underscore the importance of the antagonistic AER-FGF/CYP26B1/RA signalling module for regulating the spatiotemporally restricted gene expression along the PD limb bud axis during both initiation and SHH-dependent distal development.

## DISCUSSION

We combine transcriptional profiling with genetic analysis and mathematical modelling to analyse the gene networks regulated by SHH signalling. Although the present study agrees with a previous analysis of the impact of SHH signalling on transcriptional regulation (Vokes et al., 2008), additional conclusions can be reached as the transcriptome of *Shh*-deficient limb buds was analysed at an earlier developmental stage. By embryonic day

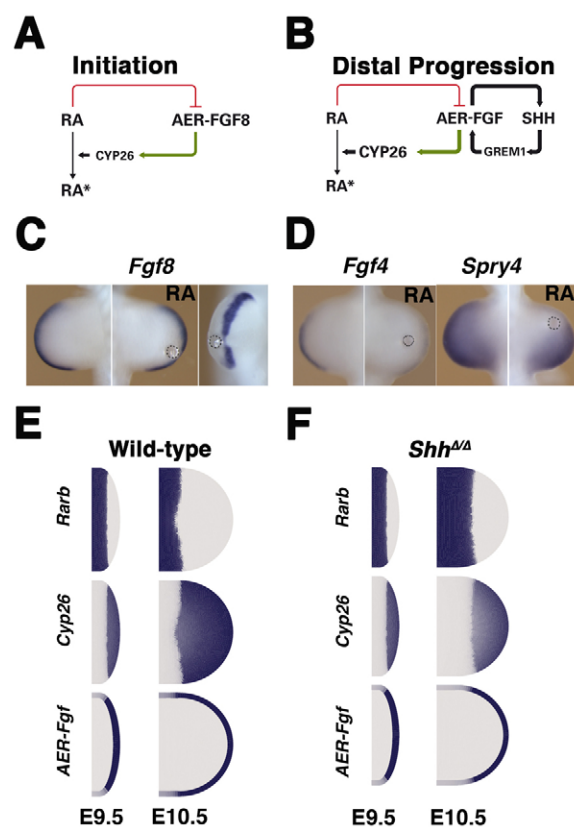


**Fig. 8. A SHH-regulated antagonistic AER-FGF/CYP26B1/RA signalling module for spatial coordination of limb bud outgrowth.** (A) Schematic representation of the postulated antagonistic signalling module during initiation limb bud development (upstream of SHH signalling). The inactivation of RA by CYP26B1-mediated hydroxylation is indicated by an asterisk (RA\*). The green arrow indicates the positive regulation of *Cyp26b1* expression by AER-FGF signalling. The red inhibitory line indicates the repression of AER-Fgf expression by high RA levels. (B) The AER-FGF mediated upregulation of *Cyp26b1* expression becomes SHH dependant during establishment of the SHH/GREM1/AER-FGF feedback loop. (C,D) Experimental verification of the postulated repression of AER-Fgfs by high RA levels. Implantation of a RA-loaded bead (1 mg/ml) into wild-type forelimb buds at E10.25 (32-33 somites, cultured for 8 hours) inhibits AER-Fgf8 ( $n=6/8$ ), *Fgf4* ( $n=7/8$ ) and *Spry4* ( $n=3/3$ ) in a differential manner. (E) Mathematical simulation of the spatial distributions of RA (*Rarb*), *Cyp26b1* and AER-Fgfs in wild-type limb buds. (F) Simulations of the *Rarb*, *Cyp26b1* and AER-Fgf distributions in *Shh*-deficient limb buds. The developmental stages indicated in E and F are approximate: E9.5 represents the SHH-independent initiation of limb bud development (A). E10.5 represents the predominantly SHH-dependent phase of limb bud development (B).

E10.5, SHH is the major driving force in the feedback signalling system that interlinks the SHH, BMP and FGF signalling pathways (Benazet et al., 2009). However, the transcriptome analysis performed here revealed an important additional function of SHH signalling for PD limb bud axis development. In fact, we identified several novel markers for the proximal limb bud mesenchyme owing to their significant upregulation and distal expansion in *Shh*-deficient limb buds. For example, *Mab2111* and *Mab2112* were identified as genes whose expressions domains can serve as additional markers for the presumptive zeugopod.

In *Shh*-deficient limb buds, the expression of molecular markers for RA activity is distally extended as a likely consequence of reduced *Cyp26b1* expression within the distal mesenchyme. Our analysis establishes that SHH-mediated upregulation of AER-FGF signalling not only propagates the SHH/GREM1/AER-FGF signalling system but also the expression of *Cyp26b1*, which in turn enhances RA clearance. To gain a better mechanistic understanding of the spatiotemporal regulation of gene expression by these interacting pathways, we simulated limb bud development in silico by translating the genetically and molecularly defined interactions into mathematical equations. These simulations reveal the existence of an antagonistic AER-FGF/CYP26B1/RA signalling module that initiates RA clearance and defines a distal domain prior to the onset of SHH signalling. Subsequently, *Cyp26b1* expression becomes dependent on SHH-mediated upregulation of AER-*Fgfs* as part of the self-regulatory SHH/GREM1/AER-FGF signalling system. The spatiotemporal simulations of PD gene expression and activity domains in wild-type and *Shh*-deficient limb buds were remarkably similar to the normal and altered gene expression domains observed in mouse limb buds.

### An antagonistic AER-FGF/CYP26B1/RA signalling module creates distal identity during onset of limb bud outgrowth

We show that the AER-FGF/CYP26B1/RA signalling module is already established during initiation of limb bud development. The key role of AER-FGFs in promoting specification and expansion of distal limb bud progenitors has been established by extensive genetic analysis in mouse embryos (Lewandoski et al., 2000; Mariani et al., 2008; Sun et al., 2002). The increase in AER-FGF signalling due to the sequential activation of *Fgf8*, *Fgf4*, *Fgf9* and *Fgf17* regulates the expansion of the mesenchymal progenitors that will give rise to progressively more distal limb skeletal elements (Mariani et al., 2008). PD limb bud identities are probably determined during progression of limb bud outgrowth round the time their differentiation is initiated (differentiation front mechanism) (Tabin and Wolpert, 2007). The complete inactivation of *Fgf8* and *Fgf4* disrupts hindlimb bud development at an early stage, while their transient expression in forelimb buds (Sun et al., 2002) suffices to initiate development of distal skeletal elements. The activation of *Cyp26b1* expression in the nascent mesenchyme suggests that a molecularly distinct pool of distal cells is already established during initiation of limb bud development and is subsequently expanded. As *Cyp26b1* expression depends on FGF signalling (this study) (Gonzalez-Quevedo et al., 2010; Hernandez-Martinez et al., 2009), limb bud mesenchymal cells that are no longer under the influence of AER-FGFs may lose *Cyp26b1* expression. In fact, *Cyp26b1* expression in the limb bud mesenchyme is more distally restricted than *Spry4*, which indicates that high levels of AER-FGFs might be required to maintain *Cyp26b1*. The AER-FGF-mediated upregulation of *Cyp26b1* expression and enhanced RA clearance is apparently important for distal limb bud development as increased RA levels are teratogenic and cause distal limb skeletal truncations (Yashiro et al., 2004; Zhou and Kochhar, 2004).

Although our study does not address the issue of whether endogenous RA is involved in specifying proximal limb bud mesenchymal identities, it provides evidence that RA is incompatible with SHH-controlled distal progression of limb bud development. However, RA may be important to restrict the length of the *Fgf*-expressing AER during the onset of forelimb bud outgrowth. RA may locally inhibit *Fgf8* expression and/or AER development via the RA-response element located in the cis-

regulatory region of the *Fgf8* locus (Zhao et al., 2009). Thus, RA might participate in defining the forelimb field and nascent bud by inhibiting *Fgf8* expression both in the trunk mesenchyme (Zhao et al., 2009) and in the overlying ectoderm (this study) by correctly scaling the *Fgf8*-expressing AER in concert with mesenchymal FGF10 and BMP4 signalling (Benazet and Zeller, 2009; Ohuchi, 1997). The higher and more general sensitivity of AER-*Fgf4* expression to RA agrees with the fact that *Fgf4* is normally only expressed after CYP26B1 has begun to inactivate RA in the distal mesenchyme (Yashiro et al., 2004). Finally, the distal expansion of proximal genes in *Cyp26b1*-deficient, *Shh*-deficient and AER-*Fgf<sup>mut</sup>* limb buds may reflect the aberrant RA activity rather than a gain of proximal identities. However, the distal expansion of the expression domains of the newly identified RA-responsive genes *Pbx1* and *Pkdcc* could have direct effects on the PD axis as their genetic inactivation alters PD limb axis development. *Pbx1*-deficient mice display anomalies of the proximal limb skeleton, while the sizes of the long limb bones are reduced in *Pkdcc*-deficient mice (Imuta et al., 2009; Selleri et al., 2001).

### SHH integrates AP and PD development during limb bud outgrowth

Our study provides mechanistic insights into the role of SHH as a node that integrates AP and PD limb axes development such that coordinated proliferation of the mesenchymal progenitors is ensured (Mariani et al., 2008; Zhu et al., 2008). Genetic evidence indicates that the AP axis is specified early and independent of the PD axis during limb bud development (Zeller et al., 2009; Zhu et al., 2008). Subsequently, the antagonistic AER-FGF/CYP26B1/RA signalling module becomes regulated by SHH as part of the self-regulatory SHH/GREM1/AER-FGF signalling system (Benazet et al., 2009). Such molecular interlinking of the AP and PD signalling systems appears essential for the dynamic and spatially coordinated regulation of gene expression and limb bud outgrowth. Last but not least, our study exemplifies how the combination of mouse genetics with in silico simulations aids in the identification of the signalling systems and interactions that control the development of complex structures such as vertebrate limbs. The possibility to simulate the key signalling interactions in both time and space begins to provide insights into the underlying interaction dynamics. For example, the genetic and functional analysis alone would not have revealed the relevance of local inhibition of AER-*Fgf8* expression by RA for restricting AER length.

The importance of FGF signalling for the expression of *Cyp26* enzymes has now been established for rather diverse developmental processes such as neurogenesis in zebrafish embryos (Gonzalez-Quevedo et al., 2010), somitogenesis in *Xenopus laevis* (Moreno and Kintner, 2004) and interdigital cell death in mouse embryos (Hernandez-Martinez et al., 2009). In fact, the FGF/CYP26/RA signalling module has been deployed repeatedly to regulate the temporally and spatially coordinated development of limb buds (this study), the neural tube (Diez del Corral et al., 2003), somites (Goldbeter et al., 2007) and germ cells (Bowles et al., 2010). During somite formation, this antagonistic signalling module has been proposed to generate sharp developmental thresholds and a bi-stable switch that governs segmentation (Goldbeter et al., 2007), which is echoed by its functions during determination of male and female germ cells (Bowles et al., 2010). Thus, this antagonistic signalling module is required for specifying distinct expression domains and/or identities during the development of rather diverse tissues and structures in vertebrate embryos.

### Acknowledgements

We acknowledge the technical support of L. D'Amato, C. Torres de los Reyes and C. Würmli, and of Drs N. Matt and E. Tiecke. A. Rosello and Dr M. Torres are thanked for the generous gift of RAA. We thank members of our groups for critical input and discussions. This research was supported by the Swiss National Science Foundation (grant numbers 31003A-112607, 31003A\_127596 to A.Z. and grant number 3100A0-113866 to R.Z.), by grants from the US National Institutes of Health (to G.R.M.) and by a grant from CREST (Core Research for Evolutional Science and Technology) of the Japan Science and Technology Corporation (to H.H.). Deposited in PMC for release after 12 months.

### Competing interests statement

The authors declare no competing financial interests.

### Supplementary material

Supplementary material for this article is available at <http://dev.biologists.org/lookup/suppl/doi:10.1242/dev.063966/-DC1>

### References

- Benazet, J. D. and Zeller, R.** (2009). Vertebrate limb development: moving from classical morphogen gradients to an integrated 4D patterning system. *Cold Spring Harb. Perspect. Biol.* **1**, a001339.
- Benazet, J. D., Bischofberger, M., Tiecke, E., Goncalves, A., Martin, J. F., Zuniga, A., Naef, F. and Zeller, R.** (2009). A self-regulatory system of interlinked signaling feedback loops controls mouse limb patterning. *Science* **323**, 1050-1053.
- Bowen, M. A., Patel, D. D., Li, X., Modrell, B., Malacko, A. R., Wang, W. C., Marquardt, H., Neubauer, M., Pesando, J. M., Francke, U. et al.** (1995). Cloning, mapping, and characterization of activated leukocyte-cell adhesion molecule (ALCAM), a CD6 ligand. *J. Exp. Med.* **181**, 2213-2220.
- Bowles, J., Feng, C. W., Spiller, C., Davidson, T. L., Jackson, A. and Koopman, P.** (2010). FGF9 suppresses meiosis and promotes male germ cell fate in mice. *Dev. Cell* **19**, 440-449.
- Capdevila, J., Tsukui, T., Rodriguez Esteban, C., Zappavigna, V. and Izpisua Belmonte, J. C.** (1999). Control of vertebrate limb outgrowth by the proximal factor Meis2 and distal antagonism of BMPs by Gremlin. *Mol. Cell* **4**, 839-849.
- Chiang, C., Litingtung, Y., Harris, M. P., Simandl, B. K., Li, Y., Beachy, P. A. and Fallon, J. F.** (2001). Manifestation of the limb prepattern: limb development in the absence of sonic hedgehog function. *Dev. Biol.* **236**, 421-435.
- Diez del Corral, R., Olivera-Martinez, I., Goriely, A., Gale, E., Maden, M. and Storey, K.** (2003). Opposing FGF and retinoid pathways control ventral neural pattern, neuronal differentiation, and segmentation during body axis extension. *Neuron* **40**, 65-79.
- Goldbeter, A., Gonze, D. and Pourquie, O.** (2007). Sharp developmental thresholds defined through bistability by antagonistic gradients of retinoic acid and FGF signaling. *Dev. Dyn.* **236**, 1495-1508.
- Gonzalez-Quevedo, R., Lee, Y., Poss, K. D. and Wilkinson, D. G.** (2010). Neuronal regulation of the spatial patterning of neurogenesis. *Dev. Cell* **18**, 136-147.
- Harfe, B. D., Scherz, P. J., Nissim, S., Tian, H., McMahon, A. P. and Tabin, C. J.** (2004). Evidence for an expansion-based temporal Shh gradient in specifying vertebrate digit identities. *Cell* **118**, 517-528.
- Hernandez-Martinez, R., Castro-Obregon, S. and Covarrubias, L.** (2009). Progressive interdigital cell death: regulation by the antagonistic interaction between fibroblast growth factor 8 and retinoic acid. *Development* **136**, 3669-3678.
- Houweling, A. C., Dildrop, R., Peters, T., Mummenhoff, J., Moorman, A. F., Ruther, U. and Christoffels, V. M.** (2001). Gene and cluster-specific expression of the Iroquois family members during mouse development. *Mech. Dev.* **107**, 169-174.
- Imuta, Y., Nishioka, N., Kiyonari, H. and Sasaki, H.** (2009). Short limbs, cleft palate, and delayed formation of flat proliferative chondrocytes in mice with targeted disruption of a putative protein kinase gene, Pkdcc (AW548124). *Dev. Dyn.* **238**, 210-222.
- Jia, Z., Agopyan, N., Miu, P., Xiong, Z., Henderson, J., Gerlai, R., Taverna, F. A., Velumian, A., MacDonald, J., Carlen, P. et al.** (1996). Enhanced LTP in mice deficient in the AMPA receptor GluR2. *Neuron* **17**, 945-956.
- Kawakami, Y., Uchiyama, Y., Rodriguez Esteban, C., Inenaga, T., Koyano-Nakagawa, N., Kawakami, H., Marti, M., Kmita, M., Monaghan-Nichols, P., Nishinakamura, R. et al.** (2009). Sall genes regulate region-specific morphogenesis in the mouse limb by modulating Hox activities. *Development* **136**, 585-594.
- Kraus, P., Fraidtenraich, D. and Loomis, C. A.** (2001). Some distal limb structures develop in mice lacking Sonic hedgehog signaling. *Mech. Dev.* **100**, 45-58.
- Lewandoski, M., Sun, X. and Martin, G. R.** (2000). Fgf8 signalling from the AER is essential for normal limb development. *Nat. Genet.* **26**, 460-463.
- MacLean, G., Abu-Abed, S., Dolle, P., Tahayato, A., Chambon, P. and Petkovich, M.** (2001). Cloning of a novel retinoic-acid metabolizing cytochrome P450, Cyp26B1, and comparative expression analysis with Cyp26A1 during early murine development. *Mech. Dev.* **107**, 195-201.
- Maksym, R. B., Tarnowski, M., Grymula, K., Tarnowska, J., Wysoczynski, M., Liu, R., Czerny, B., Ratajczak, J., Kucia, M. and Ratajczak, M. Z.** (2009). The role of stromal-derived factor-1-CXCR7 axis in development and cancer. *Eur. J. Pharmacol.* **625**, 31-40.
- Mariani, F. V., Ahn, C. P. and Martin, G. R.** (2008). Genetic evidence that FGFs have an instructive role in limb proximal-distal patterning. *Nature* **453**, 401-405.
- Mercader, N., Leonardo, E., Azpiazu, N., Serrano, A., Morata, G., Martinez, C. and Torres, M.** (1999). Conserved regulation of proximodistal limb axis development by Meis1/Hth. *Nature* **402**, 425-429.
- Mercader, N., Leonardo, E., Piedra, M. E., Martinez, A. C., Ros, M. A. and Torres, M.** (2000). Opposing RA and FGF signals control proximodistal vertebrate limb development through regulation of Meis genes. *Development* **127**, 3961-3970.
- Mercader, N., Selleri, L., Criado, L. M., Pallares, P., Parras, C., Cleary, M. L. and Torres, M.** (2009). Ectopic Meis1 expression in the mouse limb bud alters P-D patterning in a Pbx1-independent manner. *Int. J. Dev. Biol.* **53**, 1483-1494.
- Michos, O., Panman, L., Vintersten, K., Beier, K., Zeller, R. and Zuniga, A.** (2004). Gremlin-mediated BMP antagonism induces the epithelial-mesenchymal feedback signaling controlling metanephric kidney and limb organogenesis. *Development* **131**, 3401-3410.
- Minowada, G., Jarvis, L. A., Chi, C. L., Neubuser, A., Sun, X., Hacohen, N., Krasnow, M. A. and Martin, G. R.** (1999). Vertebrate Sprouty genes are induced by FGF signaling and can cause chondrodysplasia when overexpressed. *Development* **126**, 4465-4475.
- Moreno, T. A. and Kintner, C.** (2004). Regulation of segmental patterning by retinoic acid signaling during *Xenopus* somitogenesis. *Dev. Cell* **6**, 205-218.
- Nelson, C. E., Morgan, B. A., Burke, A. C., Laufer, E., DiMambro, E., Murtaugh, L. C., Gonzales, E., Tassarollo, L., Parada, L. F. and Tabin, C.** (1996). Analysis of *Hox* gene expression in the chick limb bud. *Development* **122**, 1449-1466.
- Niederreither, K., Subbarayan, V., Dolle, P. and Chambon, P.** (1999). Embryonic retinoic acid synthesis is essential for early mouse post-implantation development. *Nat. Genet.* **21**, 444-448.
- Niederreither, K., Vermot, J., Schuhbauer, B., Chambon, P. and Dolle, P.** (2002). Embryonic retinoic acid synthesis is required for forelimb growth and anteroposterior patterning in the mouse. *Development* **129**, 3563-3574.
- Ohuchi, H., Nakagawa, T., Yamamoto, A., Araga, A., Ohata, T., Ishimaru, Y., Yoshioka, H., Kuwana, T., Nohno, T., Yamasaki, M. et al.** (1997). The mesenchymal factor, FGF10, initiates and maintains the outgrowth of the chick limb bud through interaction with FGF8, an apical ectodermal factor. *Development* **124**, 2235-2244.
- Panman, L., Galli, A., Lagarde, N., Michos, O., Soete, G., Zuniga, A. and Zeller, R.** (2006). Differential regulation of gene expression in the digit forming area of the mouse limb bud by SHH and gremlin 1/FGF-mediated epithelial-mesenchymal signalling. *Development* **133**, 3419-3428.
- Platt, K. A., Michaud, J. and Joyner, A. L.** (1997). Expression of the mouse *Gli* and *Ptc* genes is adjacent to embryonic sources of hedgehog signals suggesting a conservation of pathways between flies and mice. *Mech. Dev.* **62**, 121-135.
- Selleri, L., Depew, M. J., Jacobs, Y., Chanda, S. K., Tsang, K. Y., Cheah, K. S., Rubenstein, J. L., O'Gorman, S. and Cleary, M. L.** (2001). Requirement for Pbx1 in skeletal patterning and programming chondrocyte proliferation and differentiation. *Development* **128**, 3543-3557.
- St-Jacques, B., Dassule, H. R., Karavanova, I., Botchkarev, V. A., Li, J., Danielian, P. S., McMahon, J. A., Lewis, P. M., Paus, R. and McMahon, A. P.** (1998). Sonic hedgehog signaling is essential for hair development. *Curr. Biol.* **8**, 1058-1068.
- Sun, X., Mariani, F. V. and Martin, G. R.** (2002). Functions of FGF signalling from the apical ectodermal ridge in limb development. *Nature* **418**, 501-508.
- Tabin, C. and Wolpert, L.** (2007). Rethinking the proximodistal axis of the vertebrate limb in the molecular era. *Genes Dev.* **21**, 1433-1442.
- Tamura, K., Yokouchi, Y., Kuroiwa, A. and Ide, H.** (1997). Retinoic acid changes the proximodistal developmental competence and affinity of distal cells in the developing chick limb bud. *Dev. Biol.* **188**, 224-234.
- te Welscher, P., Zuniga, A., Kuijper, S., Drenth, T., Goedemans, H. J., Meijlink, F. and Zeller, R.** (2002). Progression of vertebrate limb development through SHH-mediated counteraction of Gli3. *Science* **298**, 827-830.
- Tickle, C., Crawley, A. and Farrer, J.** (1989). Retinoic acid application to chick wing buds leads to a dose dependent reorganisation of the apical ectodermal ridge that is mediated by the mesenchyme. *Development* **106**, 691-705.
- Towers, M. and Tickle, C.** (2009). Growing models of vertebrate limb development. *Development* **136**, 179-190.
- Towers, M., Mahood, R., Yin, Y. and Tickle, C.** (2008). Integration of growth and specification in chick wing digit-patterning. *Nature* **452**, 882-886.

- Uehara, M., Yashiro, K., Takaoka, K., Yamamoto, M. and Hamada, H.** (2009). Removal of maternal retinoic acid by embryonic CYP26 is required for correct Nodal expression during early embryonic patterning. *Genes Dev.* **23**, 1689-1698.
- Verheyden, J. M. and Sun, X.** (2008). An Fgf/Gremlin inhibitory feedback loop triggers termination of limb bud outgrowth. *Nature* **454**, 638-641.
- Vokes, S. A., Ji, H., Wong, W. H. and McMahon, A. P.** (2008). A genome-scale analysis of the cis-regulatory circuitry underlying sonic hedgehog-mediated patterning of the mammalian limb. *Genes Dev.* **22**, 2651-2663.
- Wong, R. L., Chan, K. K. and Chow, K. L.** (1999). Developmental expression of Mab21l2 during mouse embryogenesis. *Mech. Dev.* **87**, 185-188.
- Yamaguchi, T. P., Bradley, A., McMahon, A. P. and Jones, S.** (1999). A Wnt5a pathway underlies outgrowth of multiple structures in the vertebrate embryo. *Development* **126**, 1211-1223.
- Yashiro, K., Zhao, X., Uehara, M., Yamashita, K., Nishijima, M., Nishino, J., Saijoh, Y., Sakai, Y. and Hamada, H.** (2004). Regulation of retinoic acid distribution is required for proximodistal patterning and outgrowth of the developing mouse limb. *Dev. Cell* **6**, 411-422.
- Zakany, J. and Duboule, D.** (2007). The role of Hox genes during vertebrate limb development. *Curr. Opin. Genet. Dev.* **17**, 359-366.
- Zeller, R., Lopez-Rios, J. and Zuniga, A.** (2009). Vertebrate limb bud development: moving towards integrative analysis of organogenesis. *Nat. Rev. Genet.* **10**, 845-858.
- Zhao, X., Sirbu, I. O., Mic, F. A., Molotkova, N., Molotkov, A., Kumar, S. and Duester, G.** (2009). Retinoic acid promotes limb induction through effects on body axis extension but is unnecessary for limb patterning. *Curr. Biol.* **19**, 1050-1057.
- Zhou, J. and Kochhar, D. M.** (2004). Cellular anomalies underlying retinoid-induced phocomelia. *Reprod. Toxicol.* **19**, 103-110.
- Zhu, J., Nakamura, E., Nguyen, M. T., Bao, X., Akiyama, H. and Mackem, S.** (2008). Uncoupling Sonic hedgehog control of pattern and expansion of the developing limb bud. *Dev. Cell* **14**, 624-632.
- Zuniga, A., Haramis, A. P., McMahon, A. P. and Zeller, R.** (1999). Signal relay by BMP antagonism controls the SHH/FGF4 feedback loop in vertebrate limb buds. *Nature* **401**, 598-602.
- Zuniga, A., Michos, O., Spitz, F., Haramis, A. P., Panman, L., Galli, A., Vintersten, K., Klasen, C., Mansfield, W., Kuc, S. et al.** (2004). Mouse limb deformity mutations disrupt a global control region within the large regulatory landscape required for Gremlin expression. *Genes Dev.* **18**, 1553-1564.